High Temporal Resolution Finite Element Simulations of the Aorta for Thoracic Impedance Cardiography

Mark Ulbrich[1], Piotr Paluchowski[1], Jens Mühlsteff[2], Steffen Leonhardt[1]

[1]Philips Chair for Medical Information Technology, RWTH Aachen University, Germany
[2]Philips Research, Eindhoven, The Netherlands

Abstract

Impedance cardiography (ICG) is a simple and cheap method to acquire hemodynamic parameters. Unfortunately, not all physiologic influences on the ICG signal have been identified, yet. In this work, the influence of the dynamics of the aorta have been analyzed using a simplified model of the human thorax with a high temporal resolution based on MRI data. Therefore, simulations have been conducted using the finite integration technique (FIT) with a temporal resolution of 125 Hz. The basis for the modeled aortic diameter change is a pulse wave propagation along the aorta derived by experimental results. It has been shown that the aorta is a major contributor to the impedance cardiogram which supports the model assumptions of Kubicek.

1. Introduction

One of the most common causes of death in Western Europe is chronic heart failure (CHF). Measures for the severity of this cardiovascular disease are hemodynamic parameters such as stroke volume (SV) or cardiac output (CO). Until now, the gold standard for measuring these parameters is the thermodilution technique which utilizes a pulmonary artery catheter. However, risks of estimating cardiac output via catheters include infections, sepsis, and arrhythmias, as well as increased morbidity and mortality [1].

An alternative method to assess hemodynamic parameters non-invasively and cost-effectively is ICG. Currently, ICG is not commonly used as diagnosis method, because it is not considered to be valid [2]. One reason is the inaccuracy of the technology itself concerning SV calculations. Another possible reason is that processes in the human body during ICG measurements are widely unknown. One way to analyze where the electrical current paths run and which tissue contributes significantly to the measurement result is to use computer simulations employing FIT [3]. Other researchers have already examined multiple sources of the ICG signal, using different approaches: some works are based on simple geometries [4], others on real anatomical data, such as MRI data [5].

Since controverse results have been obtained, the influence of one particular source for the impedance cardiogram shall be further analyzed within this work and evaluated according to its value of contribution.

2. Methods

Classical ICG analyzes the impedance of the thorax, approximating its volume by one outer cylinder with a conductivity from a mixture of tissues, containing another cylinder representing the aorta. This, of course, is an assumption which leads to modeling errors. As a result, the task is to find other models to improve the reliability of ICG measurements. In addition, it has to be clarified which physiologic sources contribute to the ICG signal and lead to its characteristic points.

This task shall be accomplished by simulations using FIT and an anatomical data set of a male human as a basis for a simplified dynamic model.

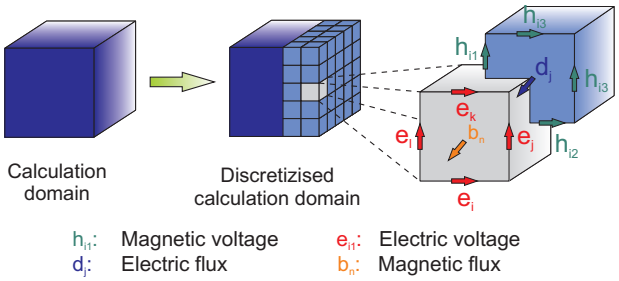

Figure 1. Finite Integration Technique.

Finite element (FE) simulations may be used to describe complex geometries by subdividing them into simple finite elements. Theses elements can be triangles or rectangles for 2D problems and tetrahedrons, pentahedrons, pyramids or hexahedrons for 3D problems. Discretization using hexahedrons is shown in fig. 1 (middle). Physical values are

assigned to the edges, surfaces and volumes of these substructures. This assignment is illustrated in fig. 1 (right) which shows 2 dual grids representing the functional principle of the FIT.

Here, electric (e) and magnetic voltages (h) are assigned to the edges while the magnetic (b) and electric fluxes (j,d) are allocated on the faces of the grids. Hence, a system of equations, the Maxwell-Grid-Equations, has to be solved for the whole calculation domain describing each cell by voltages and fluxes [6].

2.1. Modeling

Our thorax model is based on the Visible Human Project© dataset from the National Library of Medicine in Maryland, USA [7]. It provides voxel data with resolutions ranging from 1x1x1 mm to 8x8x8 mm. The origin of this data is Joseph Paul Jernigan, an executed prisoner, who has been frozen into gelatin after death. His frozen body was then cut into more than 1800 slices, so-called cryosections. These slices have been digitized by using MRI and CT with an image resolution of 4096x2700 pixels and a 24 bit color depth.

Since this dataset contains no information about dynamics, a new model had to be created using simple geometries, such as frustums, spheres and cylinders. In addition, this approach reduces simulation time. This model is shown in fig. 2.

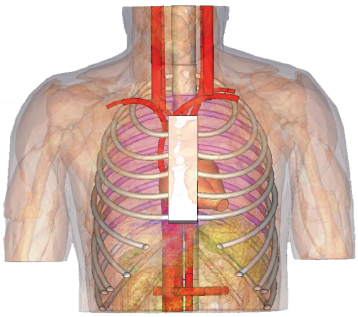

Figure 2. Thorax model developed within the reported project

It is composed of static volumes of the Visible Human dataset and new dynamic volumes: aorta, heart, vena cava, carotid vessels, rib cage and lung. The static volumes comprise the tissues fat, muscle and abdominal organs. Rebuilding all organs situated in the abdomen with the chosen procedure (importing surface polygons) would have been too complex for the desired model. In addition, the impedance change of these organs plays a subordinated role for the ICG signal during a heartbeat so that the simplification has been made that the abdominal part of the model has been filled with a uniform "tissue mixture" by using Boolean operations. An average permittivity and conductivity of all abdominal organs has then been assigned to this tissue.

The upper surface of this tissue has been used as a border for creating the lung tissue as a function of the diaphragm and rib cage position in order to increase or decrease the lung volume according to the respiratory phase. The rib cage itself has been built by using tori so that the respiration can be simulated by altering the angle of these tori around a certain axis. For simplicity, ring electrodes have been used for current injection at neck and abdomen. Of course, it is possible to use standard spot electrodes for the simulation, too. Conductivity (σ) and permittivity (ϵ_r) values for every tissue have been implemented using the data from Gabriel et al. (see tab. 2.1).

Table 1. Permittivity and conductivity values at 100 kHz [8]

	σ [S/m]	ϵ_r
Blood	0.70292	5120
Myocard	0.21511	9845.8
Bone	0.020791	227.64
Fat	0.024414	92.885
Muscle	0.36185	8089.2
Abdomen	0.2	4000
Lung	0.10735	2581.3

The static fat tissue volume serves as meta volume into which all other volumes, including the dynamic volumes, have been inserted using Boolean operations. The 3D model of blood vessels has been created using cylinders and tori in which a torus is created by rotating a circle with radius r by 360° around an axis with the distance $R > r$ located in the circle plane. It has been assumed that all blood vessels have a circular cross section throughout their entire length. For simplicity reasons, collapsed veins have not been regarded. In order to be able to simulate a wave propagation, vessels have been cut into segments whose radii can be altered based on physiological data. This approach has the advantage, that underlying physiological assumptions can be changed easily. For every expansion step of the aorta as the biggest arterial vessel, a new model has to be created since for every point in time the discretization of the simulated volume has to be recalculated due to the altered thorax geometry. The aorta has been divided into 23 segments.

2.1.1. Model dynamics

The dynamics of the aorta have been implemented based on data derived from a project in which the arterial sys-

tem has been rebuild using silicone representing an arterial model [9]. In addition, pressure and flow data has been acquired at various points on the aorta. Thus, the time development of pressure and flow for every point on the aorta could be calculated and interpolated using MATLAB®, The MathWorks, Massachusetts, USA. Using this data and the following equation, the radius for a specific segment can be adjusted:

$$R(t) = \sqrt{\frac{V_0 + V_s(t)}{\pi L}} = \sqrt{\frac{\pi R_0^2 \cdot L + \int_0^t \dot{V}_s(t)}{\pi L}} \quad (1)$$

Here, V_0 is the starting volume and $V_s(t)$ the volume calculated by the integral of the net flow $\dot{V}_s(t)$ at a certain point of time flowing through a segment indicating the volume change. Fig. 3 shows the wave propagation on the aorta by the changing vessel radius plotted against the position of the wave on the aorta and the time.

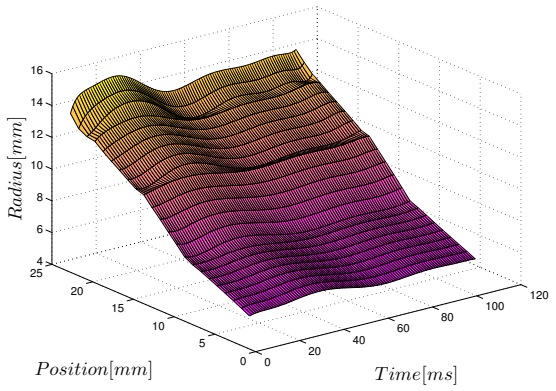

Figure 3. Aortic wave propagation

One can see that the radius change is very low due to the fast wave propagation of 5 $\frac{m}{s}$. The time resolution of the simulation comprises 103 points in time (approx. 125 Hz) within a heartbeat.

2.2. Simulation setup

We used CST EM Studio® from Computer Simulation Technology, Darmstadt, Germany to perform the simulations. All simulations have been computed on a personal computer with a 64 bit operating system, an Intel® Xeon® 5240 processor with 2 cores and 24 GB RAM. The calculation frequency has been set to 100 kHz. Since this wavelength is much higher than our measuring volume (cf. eq. 2), the low frequency electroquasistatic solver has been employed.

$$\lambda = \frac{c}{f} = \frac{300000\ \frac{km}{s}}{100\ kHz} = 3\ km \quad (2)$$

To calculate the complex impedance, a voltage source has been used to fix the voltage at the electrode sites. The current has been assessed by integrating the current density and the displacement current over a predefined face, assuming a harmonic oscillation ($\vec{D} = |D| \cdot e^{j\omega t} \cdot \vec{e}_z$). Thus, the complex current could be calculated using the following equation:

$$\underline{I} = \int_A \left(\vec{J} + \frac{\partial \vec{D}}{\partial t} \right) \cdot d\vec{A} = \int_A \left(\vec{J} + j\omega \vec{D} \right) \cdot d\vec{A} \quad (3)$$

Using a discretization density of 90 units, each model comprises 12.4 million tetrahedrons. Besides this global discretization, a finer local discretization has been used for shape changing organs in order to obtain accurate results for small geometry changes.

3. Results

In fig. 4, the results of the simulations using a dynamic aorta model is shown.

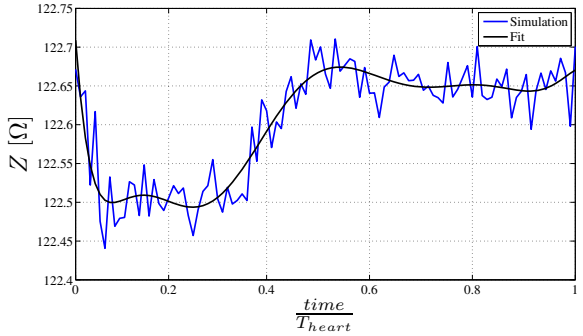

Figure 4. Simulation results with curve fit

Here, the absolute value of the impedance is plotted against the time scaled to the duration of one heartbeat. The ripple of the aortic impedance change can be explained by the changing geometry of the model due to the vessel volume change, because for every new model geometry a new mesh has to be created. This can lead to other edges or faces of the grid contributing to the results obtained by the postprocessor, even though a relatively fine discretization has been chosen. Thus, one could speak about discretization noise when talking about this phenomenon. In order to calculate the derivative, a polynomial curve fit has been computed using Matlab. The maximum impedance change caused by the aorta is 0.2 Ω.

Nevertheless, the base impedance (122.7 Ω) is too high compared to real thoracic base impedances, typically in the range of 40 Ω.

For validation purposes, the dynamic impedance simulated at 100 kHz including the volume change of the aorta has been compared to measured data of a male human. This data has been acquired using the Niccomo™ device from medis Germany, Ilmenau. Since the impedance change of the aorta does not reflect the thoracic sum impedance change, the signal has been scaled in order to be able to compare the shape of the curves.

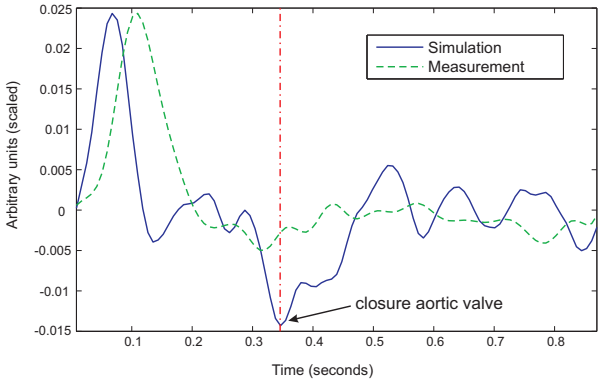

Figure 5. Simulated and measured ICG

Fig. 5 shows the fitted simulated derivative of the signal along with the measured one of a standard male human. A cross correlation analysis showed a good agreement (r = 0.75). In addition, the global minimum could be assigned to the closure of the aortic valve by comparing this curve to the temporal behaviour of the aortic pressure.

4. Discussion and conclusions

The task of this work was to analyze the influence of the aortic volume change due to a propagating blood wave in ICG measurements.

First, simulations with a high temporal resolution have been conducted using the aorta as physiologic dynamic source for the ICG signal. By a segmented aortic model, a pulse wave propagation along the aorta could be simulated. In addition, physiological data and a simple model on the basis of anatomical data have been used to produce realistic results. Thus, a resource-saving and accurate way to reproduce an impedance measurement has been implemented.

To sum up, it has been shown that although the influence of the aorta on the ICG signal is low concerning the alteration of the conductivity and thus the impedance of the human thorax, it seems that the original model of Kubicek does not really make false assumptions by taking the aorta as major contributor to the ICG signal into account. In addition, the local minimum of the ICG curve could be assigned to the aortic valve closure.

This model has of course the potential to be improved. More dynamic sources should be taken into account including erythrocyte orientation, respiration or carotid arteries and heart which have not been simulated. In addition, the simulation of one dynamic source alone allows no identification of dynamic sources according to their contribution to certain characteristic points in the ICG signal. Finally, the influence of pathologies such as edemas on the ICG signal should be analyzed in order to explain effects when measuring patients.

Acknowledgements

This work contributes to the Work Package 2 - Sensors and Parameter Extraction of the project "HeartCycle" of the European Union and has been supported by Philips Research, Eindhoven.

References

[1] Darovic G. Hemodynamic Monitoring: Invasive and Noninvasive Clinical Application. Saunders, 2002. ISBN 978-0721692937.

[2] Cotter G. Impedance cardiography revisited. Physiological Measurement 2006;27:817–827.

[3] Clemens et al. Discrete electromagnetism with the finite integration technique. Progress In Electromagnetics Research 2001;32:65–87.

[4] Kosicki J. Contributions to the impedance cardiogram waveform. Annals of Biomedical Engineering 1986;14:67–80.

[5] Patterson R. Sources of the thoracic cardiogenic electrical impedance signal as determined by a model. Medical Biological Engineering Computing 1985;23(5):411–417.

[6] Demenko A. On the equivalence of finite element and finite integration formulations. 17th Conference on the Computation of Electromagnetic Fields 2009;677–678.

[7] National Library of Medicine. The visible human project. URL `http://www.nlm.nih.gov/research/visible/visible_human.html`.

[8] Gabriel C. The dielectric properties of biological tissues. Physics in Medicine and Biology 1996;41:2231–2249.

[9] Matthys K. Pulse wave propagation in a model human arterial network: assessment of 1-d numerical simulations against in vitro measurements. Journal of Biomechanics 2007;40(15):3476–3486.

Address for correspondence:

Mark Ulbrich
Lehrstuhl für Medizinische Informationstechnik
Pauwelsstrasse 20, Room 0.11A
52074 Aachen, Germany
ulbrich@hia.rwth-aachen.de